

Steady state representation of the homogeneous cooling state of a granular gas

J. Javier Brey, M.J. Ruiz-Montero, and F. Moreno

Física Teórica, Universidad de Sevilla,

Apdo. de Correos 1065, E-41080 Sevilla, Spain

(Dated: today)

Abstract

The properties of a dilute granular gas in the homogeneous cooling state are mapped to those of a stationary state by means of a change in the time scale that does not involve any internal property of the system. The new representation is closely related with a general property of the granular temperature in the long time limit. The physical and practical implications of the mapping are discussed. In particular, simulation results obtained by the direct simulation Monte Carlo method applied to the scaled dynamics are reported. This includes ensemble averages and also the velocity autocorrelation function, as well as the self-diffusion coefficient obtained from the latter by means of the Green-Kubo representation. In all cases, the obtained results are compared with theoretical predictions.

PACS numbers: PACS Numbers: 45.70.-n,51.10.+y,05.20.Dd

I. INTRODUCTION

A granular fluid is a collection of macroscopic particles interacting via short range hard inelastic collisions. Particles move in a ballistic way between collisions and total momentum is conserved [1]. The prototypical idealized model for granular fluids is a system of inelastic smooth hard spheres or disks, with the inelasticity of collisions being described by means of a constant (independent of the relative velocity) coefficient of normal restitution. Then, in the last years the traditional methods of kinetic theory and non-equilibrium statistical mechanics have been extended to the case of inelastic collisions. Quite remarkably, it has been realized that the single feature of incorporating energy dissipation in collisions is able to provide a theoretical scheme where many of the peculiar features exhibited by real granular fluids can be tackled. This includes phenomena such as the development of strong density and temperature inhomogeneities that are not induced by the boundary conditions [2, 3], spontaneous symmetry breaking in partitioned [4, 5] and non-partitioned systems [6], segregation in systems composed of different kind of particles [7], and pattern formation [8], to cite a few examples. In most of these cases, the usefulness of a collective description of the system in terms of hydrodynamic-like equations has been verified. Such a description can only be fully understood and justified by starting from a more fundamental particle level, as considered in kinetic theory.

Due to energy dissipation in collisions, granular systems do not present a stationary, homogeneous and isotropic state similar to the equilibrium one of ordinary fluids. The simplest possible state corresponds to a freely evolving homogenous and isotropic system whose energy decays monotonically in time, the so-called homogeneous cooling state (HCS). This state plays a relevant role in order to investigate the transport properties of a granular fluid, since it provides the zeroth order in the gradients approximation when applying the Chapman-Enskog procedure to derive hydrodynamics from a given kinetic equation [9, 10]. Also, linear response around this state has been studied and formal expressions for the Navier-Stokes transport coefficients have been derived [11, 12]. They are the generalization to inelastic systems of the well-known Green-Kubo formulas. Besides their theoretical interest, they allow a direct determination of the transport coefficients from the dynamics of the system in the HCS, without introducing any additional approximation, by using numerical simulation methods.

Molecular dynamics (MD) simulation provides a method to investigate a system of particles at the most fundamental level of description. Nevertheless, when applied to a granular fluid in the HCS, several limitations show up. First, since the system is continuously cooling, the typical velocity of the particles becomes very small rather soon and numerical inaccuracies become very large. In principle, this could be solved by introducing some kind of external thermostat, but then the relationship between the original HCS and the state being actually simulated is not clear. Another possibility is to take advantage of the fact that there is no intrinsic time scale in a system of hard particles, and to rescale the velocity of all particles after every collision, so that the energy is forced to remain constant [13]. Although it seems that this method must lead to correct results for time-independent properties of the HCS, e.g. structural properties or the own scaled velocity distribution, in the infinite system limit, it is not evident how to extract from the simulation data properties of the actual dynamics of the system involving time fluctuations or two-time correlations.

Very recently, a procedure has been introduced according to which the dynamics of the system in the HCS is exactly mapped onto the dynamics around a steady state by means of a change in the time scale being used [14]. The change is independent of the state of the system. This is possible because the temperature of the HCS becomes independent of its initial value in the long time limit. This is a very strong and fundamental property of that state that has not received too much attention up to now. Then, the existence of the steady state in the scaled time representation is tied to the own physical properties of the mechanism of energy dissipation.

The second limitation of the MD simulation of a granular fluid in the HCS is associated with the fact that this state is unstable with respect to spacial long wavelength perturbations [2, 15]. This instability has been identified in the context of hydrodynamics, and an expression for the critical size of the system, beyond which it becomes unstable, has been obtained. The critical size is a function of the density and the coefficient of restitution, decreasing with the former and increasing with the latter. In practice, this implies that for high densities and/or small values of the coefficient of restitution, only very small systems can be simulated in the HCS, and undesired finite size effects might influence the results.

The aim of this paper is to investigate in detail the physical and practical implications of the steady state representation of the HCS mentioned above for a low density granular gas. Attention will be paid not only to the one-time properties of the system, but also

to two-time correlation functions. While the former can be discussed on the basis of the inelastic Boltzmann equation, the analysis of the correlation functions requires to introduce an equation for the two-particle and two-time distribution function. This is done by a direct extension of the methods used in the elastic case for out of equilibrium systems [16]. It is shown that both kind of properties can be expressed in terms of averages over the stationary state of the system. Special emphasis will be put on the relationship between the theoretical description of the system in terms of reduced distribution functions in the low density limit and the underlying N -particle dynamics. This is important in order to implement the calculation of a given property by means of the direct simulation Monte Carlo method (DSMC) [17]. It must be kept in mind that this method is designed not just as a numerical tool to solve the Boltzmann equation, but as a real N -particle dynamics simulation of a low density gas. In this sense, it is expected to provide not only the one-particle distribution function of the system, but its complete dynamical description.

One of the main practical advantages of the DSMC method is that it allows to incorporate at the level of the particle dynamics the spatial symmetry properties of the particular physical situation of interest. For instance, it is easy to restrict the dynamics of the system so that it remains homogeneous, with no possibility of developing spacial inhomogeneities. In this way, the second limitation of MD simulations of the HCS can be overcome for a low density gas with no restriction on the size of the system or the number of particles being used. The combination of this feature of the DSMC method and the steady representation of the HCS offers an almost unique way to investigate the properties of a dilute granular gas.

The plan of the paper is as follows. In Sec. II, the Boltzmann equation and some of the results for the one-particle distribution function of the HCS are shortly reviewed. The peculiar long time behavior of the temperature is indicated, and in Sec. III it is used to construct a representation of the dynamics of the system in which the distribution function of the HCS becomes time independent. It is shown that the asymptotic steady temperature is determined by an intrinsic property of the system, namely the cooling rate. Then, dynamical simulations of a system of inelastic hard disks with the DSMC method are presented, and the numerical results for the cooling rate obtained from the values of the steady temperature are compared with the existing theoretical predictions. Results for the fourth moment of the velocity distribution function are also reported. They are consistent with those obtained

previously by using the original dynamics, in which the HCS is time dependent.

Time correlation functions of dynamical variables in the HCS are addressed in Sec. IV, where their low density limit is analyzed and the relationship between their values in the original and scaled dynamics is established. The particular case of the correlation functions appearing in the Green-Kubo form of the transport coefficients of a low density gas [12] is considered. As an example, the velocity autocorrelation function, and from it the self-diffusion coefficient, are computed in Sec. V for a system of inelastic hard disks, and the results are compared with the theoretical predictions obtained by the Chapman-Enskog method in the first Sonine approximation. The paper ends with a summary and a brief discussion.

II. BASIC EQUATIONS AND THE HOMOGENEOUS COOLING STATE

We consider a system of N inelastic hard spheres ($d = 3$) or disks ($d = 2$) of mass m and diameter σ . The position and velocity coordinates of particle i at time t will be represented by $\mathbf{R}_i(t)$ and $\mathbf{V}_i(t)$, respectively. The particle dynamics consists of free streaming until a pair of particles i and j are at contact and a collision takes place. The effect of the collision is to instantaneously change the velocities of the two involved particles according to

$$\begin{aligned}\mathbf{V}_i &\rightarrow \mathbf{V}'_i \equiv b_\sigma \mathbf{V}_i = \mathbf{V}_i - \frac{1+\alpha}{2} (\hat{\boldsymbol{\sigma}} \cdot \mathbf{V}_{ij}) \hat{\boldsymbol{\sigma}} \\ \mathbf{V}_j &\rightarrow \mathbf{V}'_j \equiv b_\sigma \mathbf{V}_j = \mathbf{V}_j + \frac{1+\alpha}{2} (\hat{\boldsymbol{\sigma}} \cdot \mathbf{V}_{ij}) \hat{\boldsymbol{\sigma}},\end{aligned}\quad (1)$$

where $\mathbf{V}_{ij} = \mathbf{V}_i - \mathbf{V}_j$ is the relative velocity, $\hat{\boldsymbol{\sigma}}$ is the unit vector pointing from the center of particle j to the center of particle i at contact, and α is the coefficient of normal restitution. It is defined in the range $0 < \alpha \leq 1$ and will be considered as velocity independent along this work.

In the low density limit, it is assumed that the time evolution of the one-particle distribution function of the system $f(\mathbf{r}, \mathbf{v}, t)$ is accurately described by the inelastic Boltzmann equation [18, 19]

$$\left(\frac{\partial}{\partial t} + \mathbf{v} \cdot \frac{\partial}{\partial \mathbf{r}} \right) f(\mathbf{r}, \mathbf{v}, t) = J[f, f], \quad (2)$$

with the inelastic Boltzmann collision operator given by

$$J[f, f] \equiv \sigma^{d-1} \int d\mathbf{v}_1 \int d\hat{\boldsymbol{\sigma}} \Theta(\mathbf{g} \cdot \hat{\boldsymbol{\sigma}}) \mathbf{g} \cdot \hat{\boldsymbol{\sigma}} (\alpha^{-2} b_\sigma^{-1} - 1) f(\mathbf{r}, \mathbf{v}, t) f(\mathbf{r}, \mathbf{v}_1, t). \quad (3)$$

Here $\mathbf{g} = \mathbf{v} - \mathbf{v}_1$, Θ is the Heaviside step function, and $b_{\hat{\sigma}}^{-1}(\mathbf{v}, \mathbf{v}_1)$ is an operator replacing all the velocities \mathbf{v} and \mathbf{v}_1 appearing to its right by the precollisional values \mathbf{v}^* and \mathbf{v}_1^* given by

$$\begin{aligned}\mathbf{v}^* &\equiv b_{\hat{\sigma}}^{-1}\mathbf{v} = \mathbf{v} - \frac{1+\alpha}{2\alpha}(\hat{\sigma} \cdot \mathbf{g})\hat{\sigma}, \\ \mathbf{v}_1^* &\equiv b_{\hat{\sigma}}^{-1}\mathbf{v}_1 = \mathbf{v}_1 + \frac{1+\alpha}{2\alpha}(\hat{\sigma} \cdot \mathbf{g})\hat{\sigma}.\end{aligned}\quad (4)$$

We are using lower-case symbols to represent field variables as those appearing in the one-particle distribution function, while capital symbols are used for the particle variables. Equation (2) has a particular solution describing the HCS and having the scaling property [18]

$$f_{HCS}(\mathbf{v}, t) = n_H v_0^{-d}(t) \chi_{HCS}(\mathbf{c}), \quad (5)$$

where

$$v_0(t) = \left[\frac{2k_B T_{HCS}(t)}{m} \right]^{1/2} \quad (6)$$

is the thermal velocity and $\chi_{HCS}(\mathbf{c})$ is an isotropic function of

$$\mathbf{c} = \frac{\mathbf{v}}{v_0(t)}. \quad (7)$$

In Eq. (6), k_B is the Boltzmann constant that is usually set equal to unity in the literature of granular flows. We prefer to keep it here for dimensional reasons. The number of particles density n and the granular temperature $T(t)$ are defined, for arbitrary situations, in terms of the one-particle distribution function in the usual way,

$$n(\mathbf{r}, t) = \int d\mathbf{v} f(\mathbf{r}, \mathbf{v}, t), \quad (8)$$

$$\frac{d}{2} n(\mathbf{r}, t) k_B T(\mathbf{r}, t) = \int d\mathbf{v} \frac{1}{2} m (\mathbf{v} - \mathbf{u})^2 f(\mathbf{r}, \mathbf{v}, t), \quad (9)$$

$$n(\mathbf{r}, t) \mathbf{u}(\mathbf{r}, t) = \int d\mathbf{v} \mathbf{v} f(\mathbf{r}, \mathbf{v}, t). \quad (10)$$

Therefore, in the HCS all the time dependence of the distribution function occurs through the temperature $T_{HCS}(t)$, whose evolution equation is easily obtained from the own Boltzmann equation

$$\frac{\partial}{\partial t} T_{HCS}(t) + \zeta_{HCS}(t) T_{HCS}(t) = 0, \quad (11)$$

where the cooling rate ζ_{HCS} is given by

$$\zeta_{HCS}(t) = \frac{(1-\alpha^2)\pi^{\frac{d-1}{2}}\sigma^{d-1}n_H v_0(t)}{2\Gamma\left(\frac{d+3}{2}\right)d} \int d\mathbf{c} \int d\mathbf{c}_1 |\mathbf{c} - \mathbf{c}_1|^3 \chi_{HCS}(\mathbf{c}) \chi_{HCS}(\mathbf{c}_1). \quad (12)$$

Then, ζ_{HCS} is proportional to $T_{HCS}^{1/2}$ and, therefore, Eq. (11) can be formally integrated to get the explicit time dependence of the temperature in the HCS,

$$T_{HCS}(t) = T_{HCS}(0) \left[1 + \frac{1}{2} \zeta_{HCS}(0)t \right]^{-2}. \quad (13)$$

This expression is known as Haff's law [20] and it has the interesting property of becoming independent of the initial temperature in the long time limit. More precisely, it reduces to

$$T_{HCS} \sim 4(\bar{\zeta}t)^{-2}, \quad (14)$$

with

$$\bar{\zeta} = \frac{\zeta_{HCS}(t)}{T_{HCS}^{1/2}(t)} = \frac{v_0(t)\zeta_0}{\ell T_{HCS}^{1/2}(t)}. \quad (15)$$

In the last transformation we have introduced the time-independent dimensionless cooling rate

$$\zeta_0 = \frac{\ell \zeta_{HCS}(t)}{v_0(t)}, \quad (16)$$

where $\ell \equiv (n_H \sigma^{d-1})^{-1}$ is proportional to the mean free path. The above long time behavior of the temperature implies the existence of an asymptotic regime in which the HCS becomes independent of the initial condition or, in other words, all the homogeneous cooling states of a given system tend to converge in the long time limit. This is an exact property following from the own existence of the HCS and it will be exploited in the next Section in order to introduce a steady representation of the HCS.

Substitution of Eq. (5) into the Boltzmann equation (3) provides a closed integro-differential equation for the function $\chi_{HCS}(\mathbf{c})$,

$$\frac{\zeta_0}{2} \frac{\partial}{\partial \mathbf{c}} \cdot (\mathbf{c} \chi_{HCS}) = J_c[\chi_{HCS}, \chi_{HCS}], \quad (17)$$

$$J_c[\chi_{HCS}, \chi_{HCS}] = \int d\mathbf{c}_1 \int d\hat{\boldsymbol{\sigma}} \Theta[(\mathbf{c} - \mathbf{c}_1) \cdot \hat{\boldsymbol{\sigma}}] (\mathbf{c} - \mathbf{c}_1) \cdot \hat{\boldsymbol{\sigma}} \left[\alpha^{-2} b_{\boldsymbol{\sigma}}^{-1}(\mathbf{c}, \mathbf{c}_1) - 1 \right] \chi_{HCS}(\mathbf{c}) \chi_{HCS}(\mathbf{c}_1). \quad (18)$$

The operator $b_{\boldsymbol{\sigma}}^{-1}(\mathbf{c}, \mathbf{c}_1)$ is again defined by Eqs. (4) but substituting the velocities \mathbf{v} , \mathbf{v}_1 by \mathbf{c} , \mathbf{c}_1 .

The solution of Eq. (17) is only partially known. In particular, an expansion in Sonine polynomials has been considered. To first order, $\chi_{HCS}(\mathbf{c})$ is approximated by

$$\chi_{HCS}(\mathbf{c}) = \frac{e^{-c^2}}{\pi^{d/2}} \left[1 + a_2(\alpha) S^{(2)}(c^2) \right], \quad (19)$$

where

$$S^{(2)}(c^2) = \frac{c^4}{2} - \frac{d+2}{2}c^2 + \frac{d(d+2)}{8}. \quad (20)$$

The coefficient $a_2(\alpha)$ turns out to be proportional to the fourth cumulant of the distribution, namely

$$a_2(\alpha) = \frac{4}{d(d+2)} \left[\langle c^4 \rangle - \frac{d(d+2)}{4} \right], \quad (21)$$

$$\langle c^4 \rangle \equiv \int d\mathbf{c} c^4 \chi_{HCS}(\mathbf{c}). \quad (22)$$

When Eq. (19) is substituted into Eq. (17) a closed equation for a_2 is obtained. If nonlinear terms in a_2 are neglected in this equation, it is found [18, 21]:

$$a_2(\alpha) = \frac{16(1-\alpha)(1-2\alpha^2)}{9+24d+(8d-41)+30\alpha^2-30\alpha^3}. \quad (23)$$

In the same approximation, Eqs. (12) and (16) yield

$$\zeta_0 = \frac{\sqrt{2}\pi^{\frac{d-1}{2}}(1-\alpha^2)}{\Gamma\left(\frac{d}{2}\right)d} \left[1 + \frac{3}{16}a_2(\alpha) \right]. \quad (24)$$

The above expression for $\chi_{HCS}(\mathbf{c})$ is expected to be accurate in the thermal velocity region, i.e. for velocities c of the order of a few units. This has been confirmed by DSMC simulations of a granular gas [22].

III. STEADY STATE REPRESENTATION OF THE HCS

The long time behavior of the HCS discussed in the preceding Section, suggests that a steady representation of it can be obtained on a time scale τ defined by [14]

$$\omega_0\tau = \ln \frac{t}{t_0}, \quad (25)$$

where ω_0 and t_0 are arbitrary constants. Consistently, the velocity \mathbf{W}_i of particle i is given in the new scale by

$$\mathbf{W}_i(\tau) = \omega_0 t_0 e^{\omega_0\tau} \mathbf{V}_i(t) = \omega_0 t \mathbf{V}_i(t). \quad (26)$$

The particle dynamics in these variables consists of an accelerating streaming between collisions,

$$\begin{aligned} \frac{\partial}{\partial\tau} \mathbf{R}_i(\tau) &= \mathbf{W}_i(\tau), \\ \frac{\partial}{\partial\tau} \mathbf{W}_i(\tau) &= \omega_0 \mathbf{W}_i(\tau), \end{aligned} \quad (27)$$

while the effect of a collision between particles i and j is to instantaneously modify their velocities accordingly with the same rules as given in Eqs. (1), i.e.

$$\begin{aligned}\mathbf{W}_i &\rightarrow \mathbf{W}'_i \equiv b_{\boldsymbol{\sigma}} \mathbf{W}_i = \mathbf{W}_i - \frac{1+\alpha}{2} (\hat{\boldsymbol{\sigma}} \cdot \mathbf{W}_{ij}) \hat{\boldsymbol{\sigma}} \\ \mathbf{W}_j &\rightarrow \mathbf{W}'_j \equiv b_{\boldsymbol{\sigma}} \mathbf{W}_j = \mathbf{W}_j + \frac{1+\alpha}{2} (\hat{\boldsymbol{\sigma}} \cdot \mathbf{W}_{ij}) \hat{\boldsymbol{\sigma}}.\end{aligned}\quad (28)$$

Of course, this invariance of the collision rules is a consequence of the instantaneous character of the hard collisions or, in other words, of the absence of an intrinsic time scale for hard particles. In the τ time scale, the Boltzmann equation (2) takes the form

$$\left(\frac{\partial}{\partial \tau} + \omega_0 \frac{\partial}{\partial \mathbf{w}} \cdot \mathbf{w} + \mathbf{w} \cdot \frac{\partial}{\partial \mathbf{r}} \right) \tilde{f}(\mathbf{r}, \mathbf{w}, t) = J[\tilde{f}, \tilde{f}]. \quad (29)$$

Here J is the same collision operator as in Eq. (3) with but substituting the velocities \mathbf{v}, \mathbf{v}_1 by \mathbf{w}, \mathbf{w}_1 , and the scaled one-particle distribution function is

$$\tilde{f}(\mathbf{r}, \mathbf{w}, t) = (\omega_0 t)^{-d} f(\mathbf{r}, \mathbf{v}, t). \quad (30)$$

Therefore, the only modification of the Boltzmann equation is that a new term appears in the streaming part of the equation, as expected because of Eqs. (27). This term has the same form as some thermostats introduced more or less artificially in order to allow the system to have a stationary state; however here it arises solely from a change in the time scale.

Let us assume now that the system is initially in the HCS and that it remains in it along its time evolution. This implies to suppress the possibility that the system spontaneously develops spatial inhomogeneities due to the existence of a long wavelength hydrodynamic instability, the so-called clustering instability [2, 15]. It is worth to stress that this effect is also present in the low density description provided by the Boltzmann equation [22, 23]. In principle, the instability can be avoided by considering small enough systems, but this might lead to the presence of undesired finite size effects, especially for small values of the coefficient of restitution α . Nevertheless, at the level of description provided by the Boltzmann equation, this can be formally accomplished by restricting ourselves to consider the homogeneous form of Eq. (29). Then, a scaled temperature $\tilde{T}_{HCS}(\tau)$ can be defined by

$$\frac{d}{2} n_H k_B \tilde{T}_{HCS}(\tau) = \int d\mathbf{w} \frac{1}{2} m w^2 \tilde{f}_{HCS}(\mathbf{w}, \tau), \quad (31)$$

where $\tilde{f}_{HCS}(\mathbf{w}, \tau)$ is the scaled one-particle distribution of the HCS. An evolution equation for this temperature is easily obtained by using Eq. (11),

$$\left(\frac{\partial}{\partial \tau} - 2\omega_0\right)\tilde{T}_{HCS}(\tau) = -\bar{\zeta}\tilde{T}_{HCS}^{3/2}(\tau). \quad (32)$$

The solution of this equation is

$$\tilde{T}_{HCS}(\tau) = \left(\frac{2\omega_0}{\bar{\zeta}}\right)^2 \left[1 + \left(\frac{2\omega_0}{\bar{\zeta}\tilde{T}_{HCS}^{1/2}(0)} - 1\right)e^{-\omega_0\tau}\right]^{-2}. \quad (33)$$

It follows that any initial value of the temperature tends to a final steady value given by

$$\tilde{T}_{st} = \left(\frac{2\omega_0}{\bar{\zeta}}\right)^2. \quad (34)$$

As discussed above, this result only holds as long as the system stays indefinitely in the HCS. By means of Eq. (15), it can also be expressed in the equivalent form

$$\zeta_0 = \frac{2\omega_0\ell}{\tilde{v}_{0,st}}, \quad (35)$$

with

$$\tilde{v}_{0,st} = \left(\frac{2k_B\tilde{T}_{st}}{m}\right)^{1/2}. \quad (36)$$

Therefore, $\omega_0/\tilde{v}_{0,st}$ is independent of ω_0 and proportional to an intrinsic property of the system, namely the dimensionless cooling rate ζ_0 .

Moreover, once the scaled temperature has reached its steady value, the scaled distribution function has the time independent form

$$\tilde{f}_{st}(\mathbf{w}) = n_H\tilde{v}_{0,st}^{-d}\chi_{HCS}(\tilde{\mathbf{c}}), \quad \tilde{\mathbf{c}} = \frac{\mathbf{c}}{\tilde{w}_{0,st}} = \frac{\tilde{v}_{0,st}}{v_0(t)}\mathbf{v}. \quad (37)$$

Upon writing the last equality for $\tilde{\mathbf{c}}$, we have taken into account the asymptotic form of $T_{HCS}(t)$ given in Eq. (14). The existence of a steady solution of Eq. (29) is enabled by the term proportional to ω_0 , so that the acceleration between collisions is able to balance the loss of energy in them. In order to avoid misunderstandings, it must be noted that the fact that the system is in the HCS does not imply by itself that the temperature in the scaled variables takes its steady value. This only happens in the long time limit. However, what is relevant is that there is a mapping between the steady state in the scaled representation and the associated HCS, for arbitrary value of the parameter ω_0 . Of course, for any arbitrary state of the system, it is possible to relate every property in the original variables with the

corresponding (scaled) property in the scaled representation, but attention will be restricted in the following to the HCS.

In order to confirm the practical usefulness of the steady representation, we have carried out DSMC simulations [17] of a low density granular gas whose dynamics is defined by Eqs. (27) and (28). This N -particle simulation algorithm is known to be consistent with the Boltzmann equation, in the sense that it provides numerical solutions of the equation. But the results coming from this kind of simulations go much further and cover all the properties of a dilute gas. This includes, in particular, fluctuations and non-equilibrium correlations, although the precise relationship between the simulation algorithm and the theory following from a description of the system in the context of kinetic theory, or non-equilibrium statistical mechanics, has not been established yet. In fact, the method tries to mimic, by means of a Markov process, the dynamics of a low density gas by uncoupling the streaming motion of the particles, given by Eqs. (27), and collisions during a small enough time interval, and also by neglecting velocity correlations in collisions. This is done independently of the number N of particles being simulated (and, therefore, of their number density). In practice, this is implemented by dividing the coordinate space into cells of size smaller than the mean free path, and considering that all pairs of particles in the same cell can collide with a probability proportional to their relative velocity.

One of the main technical advantages of DSMC, as compared with other particle simulation methods, is that it allows to incorporate in the simulation algorithm the eventual symmetry properties of the particular physical situation of interest. The most trivial effect of this is the possibility of increasing the numerical statistics of the results, but it also permits to force the system to stay with a given symmetry, by eliminating from the dynamics the degrees of freedom associated with the “irrelevant” directions. For instance, for our present purposes we want the system to stay in the HCS, so that no spatial instabilities can be developed in any direction, and at the same time we want to avoid the introduction of finite size effects. This can be accomplished by simulating the N -particle dynamics associated with the *homogeneous* Boltzmann equation. The way of implementing this in the simulation is by considering only one cell, i.e. any pair of particles in the system can collide and no attention is paid to their positions. Since the technical details of the method have been extensively discussed in the literature [17, 24], they will not be reproduced here.

The simulations we will present in the following correspond to a two-dimensional system

of hard disks, i.e. $d = 2$. As already discussed, no boundary conditions are needed since we are simulating homogeneous situations and the positions of the particles play no role. For the same reason, there is no system size to be specified. Moreover, the numerical data we will report have been averaged over a number of trajectories, typically of the order of a few thousands. The number of particles in the system is $N = 10^4$, but we insist on that it has only a statistical meaning, since the dynamics of the system being used in the simulation corresponds always by construction to that of a low density gas.

Accordingly with the scenario we have developed, the simulation of a low density gas whose underlying particle dynamics is defined by Eqs. (27) and (28), is expected to yield a steady state after a relatively short transient period. Averages of properties in the steady state are simply related with the (time dependent) properties of the HCS. In this way, the difficulties associated with the fast cooling of the fluid when described in terms of the actual variables, leading very soon to numerical inaccuracies, are overcome. One technical point requiring some attention is that the total momentum is unstable in the mapped representation for all sizes of the system [14]. Round-off numerical errors lead to the presence of nonzero total momentum that grow very quickly due to the instability. This is easily avoided by calculating the total momentum at each simulation step and subtracting it evenly from the momentum of each particle.

In the results to be reported in the following, the unit of time is given by $\ell[2k_B\tilde{T}(0)/m]^{-1/2}$, the unit of length is ℓ , the unit of mass is m , and k_B has been set equal to unity. In Fig. 1 the evolution of the scaled temperature \tilde{T} is plotted as a function of the time τ for several values of α , namely $\alpha = 0.5, 0.6, 0.7,$ and 0.9 . The value of ω_0 used in each case is $\omega_0 = \bar{\zeta}\tilde{T}(0)^{1/2}/2$, with $\bar{\zeta}(\alpha)$ approximated by its estimate in the first Sonine approximation as given by Eqs. (15) and (24). If this latter expression were exact, the final steady temperature would be exactly the same as the initial one. The observed behavior is consistent with the theoretical predictions. In all the cases the temperature fluctuates around a steady value after an initial transient time. In the original time scale, this corresponds to the regime in which the granular temperature has already reached its asymptotic form given in Eq. (14). The steady value is very close to the initial temperature, as expected, although a small deviation is clearly identified for $\alpha = 0.5$, indicating the approximated nature of expression (24) for ζ_0 . It is also seen in the figure that the amplitude of the long time temperature fluctuations increases as the value of the coefficient of restitution

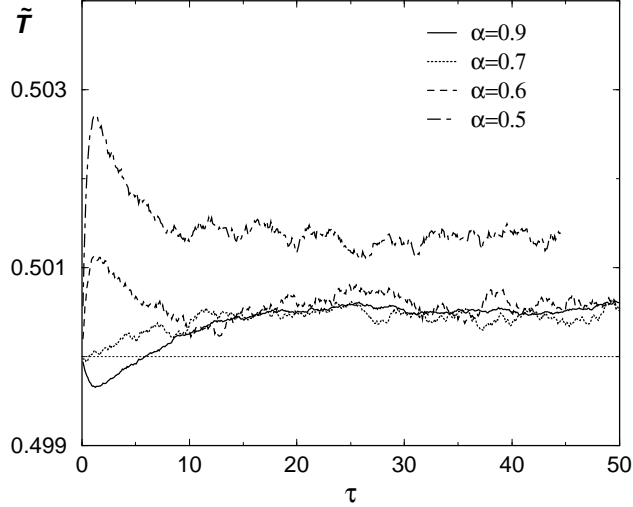


FIG. 1: Evolution of the scaled temperature \tilde{T} as a function of the scaled time τ . Units are defined in the main text. The different line styles correspond to different values of α as indicated in the figure.

decreases, i.e. as the system is more inelastic. This is due to the change of the shape of the velocity distribution function and also to the presence of velocity correlations in the HCS that are generated by the N -particle dynamics of the system, even in the low density limit. This will be discussed in more detail elsewhere.

From the values of \tilde{T}_{st} , the cooling rate ζ_0 can be obtained as a function of α by means of Eq. (35). In Fig. 2 these numerical results are compared with the theoretical prediction given by Eq. (24). As already indicated by the weak dependence on α of the steady temperature in Fig. 1, there is a very good agreement. The discrepancy observed in the latter for $\alpha = 0.5$ can not be made out on the scale used in Fig. 2.

Since the steady velocity distribution has the same form as χ_{HCS} , the steady representation also provides very accurate data for it. As an example, in Fig. 3 the coefficient a_2 defined by Eq. (21) is plotted as a function of the coefficient of restitution and compared with the approximated expression given by Eq. (23). In this case, a small but systematic deviation is observed. The results presented so far in the above three figures are consistent, and physically equivalent, to those obtained previously by carrying out DSMC simulations in the actual variables of the system, i.e. by dealing directly with the time-dependent HCS [22]. The main advantage of the present representation is that it reduces the statistical uncertainties by introducing a steady state that maps exactly into the HCS. In the next

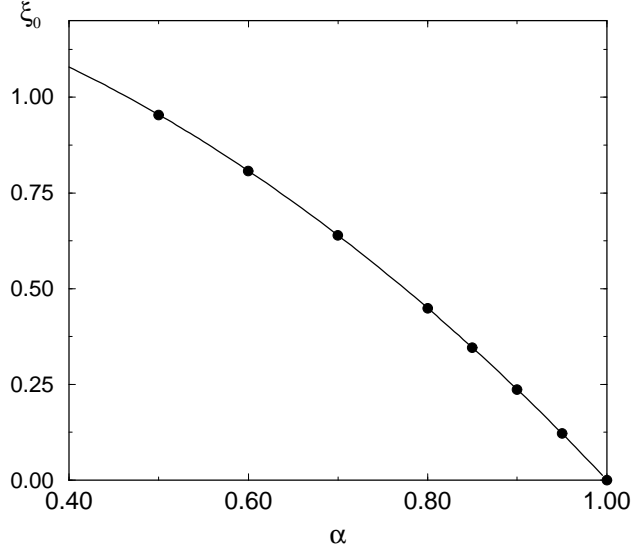


FIG. 2: The dimensionless cooling rate ζ_0 as a function of the coefficient of restitution α . The symbols are the values obtained from the simulations, while the solid line is the theoretical prediction in the first Sonine approximation.

Section, it will be shown that the scaling is also useful to study time correlation functions.

IV. AVERAGES AND TIME-CORRELATION FUNCTIONS IN THE STEADY REPRESENTATION

Consider a phase function of the form

$$A(\Gamma) = \sum_{i=1}^N a(\mathbf{R}_i, \mathbf{V}_i), \quad (38)$$

where Γ denotes a point in the phase space of the system and $a(\mathbf{R}_i, \mathbf{V}_i)$ is a given one-particle dynamical variable. The average value of A at time t is

$$\langle A; t \rangle \equiv \int d\Gamma A(\Gamma, t) \rho(\Gamma, 0) \equiv \int d\Gamma A(\Gamma) \rho(\Gamma, t). \quad (39)$$

Here $\rho(\Gamma, t)$ is the N -particle distribution function of the system at time t . This equation is equivalent to

$$\langle A; t \rangle = \int d\mathbf{r} \int d\mathbf{v} a(\mathbf{r}, \mathbf{v}) f(\mathbf{r}, \mathbf{v}, t), \quad (40)$$

that, using the scaling defined by Eqs. (25) and (30), can also be expressed as

$$\langle A; t \rangle = \int d\mathbf{r} \int d\mathbf{w} a[\mathbf{r}, (\omega_0 t)^{-1} \mathbf{w}] \tilde{f}(\mathbf{r}, \mathbf{w}, \tau). \quad (41)$$

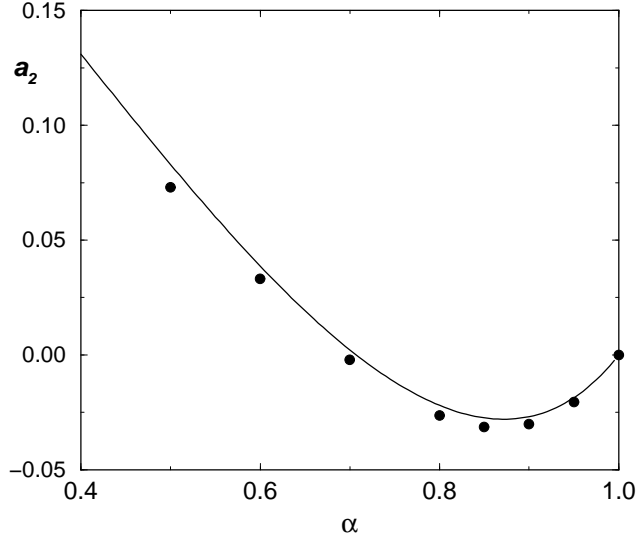


FIG. 3: Coefficient a_2 defined in Eq. (21) as a function of the coefficient of restitution α . The symbols are from the DSMC simulations, while the solid line is the theoretical prediction discussed in the main text.

Suppose now a dilute system in the HCS. It has been established in Sec. III that in the long time limit, the scaled distribution function tends to the steady form $\tilde{f}_{st}(\mathbf{w})$ given by Eq. (37), so that Eq. (41) becomes

$$\langle A; t \rangle_{HCS} = \int d\mathbf{r} \int d\mathbf{w} a \left[\mathbf{r}, \frac{v_0(t)}{\tilde{v}_{0,st}} \mathbf{w} \right] \tilde{f}_{st}(\mathbf{w}). \quad (42)$$

This is the low density limit of

$$\langle A; t \rangle_{HCS} = \int d\tilde{\Gamma} \tilde{A}(\tilde{\Gamma}) \tilde{\rho}_{st}(\tilde{\Gamma}), \quad (43)$$

where $\tilde{\Gamma} = \{\mathbf{R}_i, \mathbf{W}_i; i = 1, \dots, N\}$,

$$\tilde{A}(\tilde{\Gamma}) = \sum_{i=1}^N a \left[\mathbf{R}_i, \frac{v_0(t)}{\tilde{v}_{0,st}} \mathbf{W}_i \right], \quad (44)$$

and $\tilde{\rho}_{st}(\tilde{\Gamma})$ is the scaled N -particle distribution of the steady state.

In this way, averages in the HCS are exactly mapped onto averages in the steady state of the scaled dynamics. It could be thought that since Eq. (42) has been obtained as the long time limit of Eq. (41) for the HCS, its validity is somewhat restricted to very low actual temperatures $T_{HCS}(t)$. Nevertheless, this is not the case, because formally the initial temperature $T_{HCS}(0)$ can be as large as wanted and, consequently, Eq. (42) can be

applied at any temperature $T_{HCS}(t)$. In fact, it is easily verified that the same equation can be derived from the particularization of Eq. (40) to the HCS by making the change of variable $\mathbf{w} = \tilde{v}_{0,st}\mathbf{c}$, without introducing any long time limit. Of course, the difference is that in this latter case $T_{HCS}(t)$, present in Eq. (42) through $v_0(t)$, can not be substituted by its asymptotic form.

Next, let us consider time correlation functions in the HCS defined by

$$C_{AB}(t, t') \equiv \langle A(t)B(t'); 0 \rangle_{HCS} - \langle A; t \rangle_{HCS} \langle B; t' \rangle_{HCS}, \quad (45)$$

with

$$\langle A(t)B(t'); 0 \rangle_{HCS} \equiv \int d\Gamma A(\Gamma, t)B(\Gamma, t')\rho_{HCS}(\Gamma, 0) \quad (46)$$

and it is assumed that $t > t' > 0$. The phase functions $A(\Gamma)$ and $B(\Gamma)$ are the sum of one-particle dynamical variables, i.e. A is again given by Eq. (38) and

$$B(\Gamma) = \sum_{i=1}^N b(\mathbf{R}_i, \mathbf{V}_i). \quad (47)$$

Then, Eq. (45) can be rewritten in the equivalent form

$$C_{AB}(t, t') = \int d\mathbf{r}_1 \int d\mathbf{v}_1 \int d\mathbf{r}'_1 \int d\mathbf{v}'_1 a(\mathbf{r}_1, \mathbf{v}_1) b(\mathbf{r}'_1, \mathbf{v}'_1) h_{1/1}(\mathbf{r}_1, \mathbf{v}_1, t; \mathbf{r}'_1, \mathbf{v}'_1, t'), \quad (48)$$

where $h_{1/1}$ is the two-particle two-time correlation function of the HCS defined by [16]

$$h_{1/1}(\mathbf{r}_1, \mathbf{v}_1, t; \mathbf{r}'_1, \mathbf{v}'_1, t') \equiv f_{1/1}(\mathbf{r}_1, \mathbf{v}_1, t; \mathbf{r}'_1, \mathbf{v}'_1, t') - f_{HCS}(\mathbf{v}_1, t) f_{HCS}(\mathbf{v}'_1, t'). \quad (49)$$

Here $f_{1/1}$ is the two-particle two-time reduced distribution function of the HCS,

$$\begin{aligned} f_{1/1}(\mathbf{r}_1, \mathbf{v}_1, t; \mathbf{r}'_1, \mathbf{v}'_1, t') &\equiv \sum_{i=1}^N \sum_{j=1}^N \int d\Gamma \rho_{HCS}(\Gamma) \delta[\mathbf{r}_1 - \mathbf{R}_i(t)] \delta[\mathbf{v}_1 - \mathbf{V}_i(t)] \\ &\times \delta[\mathbf{r}'_1 - \mathbf{R}_j(t')] \delta[\mathbf{v}'_1 - \mathbf{V}_j(t')]. \end{aligned} \quad (50)$$

In the low density limit, and by using the same kind of assumptions as needed to derive the Boltzmann equation, it is possible to obtain a formal expression for $h_{1/1}$ involving only the steady one-particle distribution function [16]. A sketch of the calculations is given in the Appendix A. When this expression is substituted into Eq. (48) it is obtained:

$$C_{AB}(t, t') = \int d\mathbf{r}_1 \int d\mathbf{w}_1 \tilde{f}_{st}(\mathbf{w}_1) a \left[\mathbf{r}_1, \frac{v_0(t)}{\tilde{v}_{0,st}} \mathbf{w}_1, \tau - \tau_1 \right] b \left[\mathbf{r}_1, \frac{v_0(t')}{\tilde{v}_{0,st}} \mathbf{w}_1 \right]. \quad (51)$$

The time dependence of the dynamical variable a is given by

$$a(\mathbf{r}_1, \mathbf{w}_1, \tau) = e^{\tau \bar{L}_B(\mathbf{w}_1)} a(\mathbf{r}_1, \mathbf{w}_1). \quad (52)$$

where $\bar{L}_B(\mathbf{w}_1)$ is the adjoint of the linearized Boltzmann operator around the steady state in the scaled dynamics,

$$\bar{L}_B(\mathbf{w}_1) = \mathbf{w}_1 \cdot \frac{\partial}{\partial \mathbf{r}_1} + \bar{\Lambda}_{st}(\mathbf{w}_1), \quad (53)$$

$$\bar{\Lambda}_{st} = \omega_0 \mathbf{w}_1 \cdot \frac{\partial}{\partial \mathbf{w}_1} + \bar{K}_{st}(\mathbf{w}_1), \quad (54)$$

$$\bar{K}_{st}(\mathbf{w}_1) = \sigma^{d-1} \int d\mathbf{w}_2 \tilde{f}_{st}(\mathbf{w}_2) \int d\hat{\sigma} \Theta(\mathbf{w}_{12} \cdot \hat{\sigma}) \mathbf{w}_{12} \cdot \hat{\sigma} [b_\sigma(\mathbf{w}_1, \mathbf{w}_2) - 1] (1 + \mathcal{P}_{12}). \quad (55)$$

The operator \mathcal{P}_{12} interchanges the subindexes 1 and 2 to its right. Of course, if the dynamical variable a does not depend on the position \mathbf{r} , $\bar{L}_B(\mathbf{w}_1)$ can be substituted by $\bar{\Lambda}_{st}(\mathbf{w}_1)$ in Eq. (52).

In the particular, but quite frequent case that a and b are homogeneous functions of the velocity of degree q_1 and q_2 , respectively, i.e.

$$\begin{aligned} a \left[\mathbf{r}_1, \frac{v_0(t)}{\tilde{v}_{0,st}} \mathbf{w}_1 \right] &= \left[\frac{v_0(t)}{\tilde{v}_{0,st}} \right]^{q_1} a(\mathbf{r}_1, \mathbf{w}_1), \\ b \left[\mathbf{r}_1, \frac{v_0(t')}{\tilde{v}_{0,st}} \mathbf{w}_1 \right] &= \left[\frac{v_0(t')}{\tilde{v}_{0,st}} \right]^{q_2} b(\mathbf{r}_1, \mathbf{w}_1), \end{aligned} \quad (56)$$

the time-correlation function becomes

$$C_{AB}(t, t') = \frac{v_0^{q_1}(t) v_0^{q_2}(t')}{\tilde{v}_{0,st}^{q_1+q_2}} \int d\mathbf{r}_1 \int d\mathbf{w}_1 \tilde{f}_{st}(\mathbf{w}_1) a(\mathbf{r}_1, \mathbf{w}_1, \tau - \tau_1) b(\mathbf{r}_1, \mathbf{w}_1). \quad (57)$$

In the context of the steady representation of the HCS of a low density granular gas as discussed in this paper, the relevant point of the above analysis is the following: suppose that a property of the gas can be expressed in terms of the time correlation function

$$\langle a(\tau) b \rangle_{st} \equiv \int d\mathbf{r} \int d\mathbf{v} \tilde{f}_{st}(\mathbf{v}) a(\mathbf{r}, \mathbf{v}, \tau) b(\mathbf{r}, \mathbf{v}), \quad (58)$$

with the time-dependence of $a(\mathbf{r}, \mathbf{v}, \tau)$ given by Eq. (52). A slight modification of the preceding discussion shows that this is the low density limit of

$$C_{AB,st}(\tau) = \langle A(\tau) B; 0 \rangle_{st} - \langle A \rangle_{st} \langle B \rangle_{st}, \quad (59)$$

where

$$\langle A \rangle_{st} = \int d\Gamma \rho_{st}(\Gamma) A(\Gamma), \quad \langle B \rangle_{st} = \int d\Gamma \rho_{st}(\Gamma) B(\Gamma), \quad (60)$$

$$\langle A(\tau)B; 0 \rangle_{st} = \int d\Gamma \rho_{st}(\Gamma) A(\Gamma, \tau) B(\Gamma), \quad (61)$$

with $A(\Gamma)$ and $B(\Gamma)$ given by Eqs. (38) and (47), respectively. Besides, $A(\Gamma, \tau)$ is generated from $A(\Gamma)$ by the dynamics defined by Eqs. (27) and (28), and $\rho_{st}(\Gamma)$ is the N -particle distribution function of the steady state eventually reached by the system. Although the existence of this state is not rigorously proven, it is supported by the discussion carried in Sec. III at the level of the Boltzmann equation and also by Molecular Dynamics simulations [14, 25]. The DSMC method provides an efficient tool to generate the N -particle dynamical representation of a dilute gas, that is consistent with the Boltzmann equation. In summary, it allows the direct evaluation of Eq. (59) in the low density limit, where it is equivalent to Eq. (58).

An important application of the above ideas is the evaluation of the Navier-Stokes transport coefficients of a dilute granular gas composed of hard spheres or disks. In refs. [12, 26, 27], these coefficients were derived from the inelastic Boltzmann equation by means of the Chapman-Enskog procedure, eigenfunctions expansions, and linear response theory, finding equivalent results. The expressions of all the transport coefficients are proportional to time integrals of correlation functions of the form

$$D_{ab}(s) = \int d\mathbf{c}_1 \chi_{HCS}(\mathbf{c}_1) a(\mathbf{c}_1, s) b(\mathbf{c}_1), \quad (62)$$

with the time dependence of $a(\mathbf{c}, s)$ determined by

$$a(\mathbf{c}_1, s) = e^{s\bar{\Lambda}_c(\mathbf{c}_1)} a(\mathbf{c}_1), \quad (63)$$

$$\bar{\Lambda}_c(\mathbf{c}_1) = \int d\mathbf{c}_2 \chi_{HCS}(\mathbf{c}_2) \int d\hat{\boldsymbol{\sigma}} \Theta(\mathbf{c}_{12} \cdot \hat{\boldsymbol{\sigma}}) \mathbf{c}_{12} \cdot \hat{\boldsymbol{\sigma}} [b_{\boldsymbol{\sigma}}(\mathbf{c}_1, \mathbf{c}_2) - 1] (1 + \mathcal{P}_{12}) + \frac{\zeta_0}{2} \mathbf{c}_1 \cdot \frac{\partial}{\partial \mathbf{c}_1}. \quad (64)$$

Finally, the time scale s is defined as

$$s = \int_0^t dt' \frac{v_0(t')}{\ell}. \quad (65)$$

Although the above representation is appropriate for formal manipulations, for computational purposes the dynamics associated with the operator $\bar{\Lambda}_c$ presents the technical complication that it involves the cooling rate ζ_0 , that therefore must be known a priori instead of being determined by the own simulation, as it is the case for the scaled dynamics being used in the present paper. For this reason, it is convenient to transform Eq. (62) by writing it in terms of that dynamics. This is easily accomplished by introducing

$$\tau = \frac{\zeta_0}{2\omega_0} s, \quad \mathbf{w} = \frac{2\omega_0 \ell}{\zeta_0} \mathbf{c} = \tilde{v}_{0,st} \mathbf{c}. \quad (66)$$

Then, for an arbitrary function $g(\mathbf{c})$ it is obtained

$$s\bar{\Lambda}_c g(\mathbf{c}) = \tau \bar{\Lambda}_{st} g\left(\frac{\mathbf{w}}{\tilde{v}_{0,st}}\right), \quad (67)$$

where $\bar{\Lambda}_{st}$ is the operator defined by Eq. (54). It follows that Eq. (62) is the same as

$$D_{ab}(s) = \frac{1}{N} \left\langle a\left(\frac{\mathbf{v}}{\tilde{v}_{0,st}}, \tau\right) b\left(\frac{\mathbf{v}}{\tilde{v}_{0,st}}\right) \right\rangle_{st}, \quad (68)$$

where we use the notation introduced in Eq. (58). The above result relates the expression of the transport coefficients of a dilute granular gas, as obtained from the Boltzmann equation for the one-particle distribution function, with the low density limit of time-correlation functions in the N -particle dynamics, computed in the steady state of the scaled representation introduced in Sec. III.

V. SELF-DIFFUSION

In ref. [28], the expression of the self-diffusion coefficient D of a dilute inelastic gas of hard particles has been derived from the Boltzmann-Lorentz equation by the Chapman-Enskog procedure. In Appendix B it is shown that the results reported in [28] can be expressed in the form

$$\begin{aligned} D &= \frac{v_0(t)\ell}{d} \int_0^\infty ds \int d\mathbf{c} \chi_{HCS}(\mathbf{c}) \mathbf{c}(s) \cdot \mathbf{c} \\ &= \frac{v_0(t)}{\tilde{v}_{0,st} N d} \int_0^\infty \langle \mathbf{w}(t) \cdot \mathbf{w} \rangle_{st}. \end{aligned} \quad (69)$$

In the last transformation we have used Eq. (68). In fact, this is an special case, since the time dependence of $\mathbf{c}(s)$ is not given by the linearized Boltzmann collision operator $\bar{\Lambda}_c$ as in Eq. (63), but by the Lorentz-Boltzmann one $\bar{\Lambda}_{BL,c}(\mathbf{c})$, defined in Eq. (B11),

$$\mathbf{c}(s) = e^{s\bar{\Lambda}_{BL,c}(\mathbf{c})} \mathbf{c}. \quad (70)$$

Consequently, in Eq. (69) it is

$$\mathbf{w}(\tau) = e^{\tau\bar{\Lambda}_{BL,st}(\mathbf{w})} \mathbf{w}, \quad (71)$$

$$\bar{\Lambda}_{BL,st}(\mathbf{w}) = \sigma^{d-1} \int d\mathbf{w}_1 \tilde{f}_{st}(\mathbf{w}_1) \int d\hat{\boldsymbol{\sigma}} \Theta(\mathbf{g} \cdot \hat{\boldsymbol{\sigma}}) \mathbf{g} \cdot \hat{\boldsymbol{\sigma}} [b_\sigma(\mathbf{w}, \mathbf{w}_1) - 1] + \frac{\zeta_0}{2} \mathbf{w} \cdot \frac{\partial}{\partial \mathbf{w}}. \quad (72)$$

Nevertheless, all the reasonings in Sec. IV and Appendix A can be easily adapted to the present case. The only, but relevant, difference, is that now the expression $\langle \mathbf{w}(t) \cdot \mathbf{w} \rangle_{st}$ is

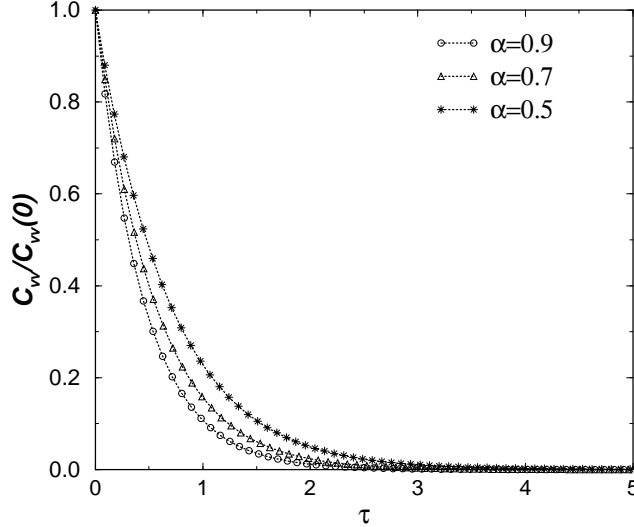


FIG. 4: Time evolution of the normalized velocity autocorrelation function $C_{vv}(\tau)/C_{vv}(0)$ as a function of the scaled time τ . The results for three different values of the coefficient of restitution α are shown, as indicated in the figure.

the low density limit of

$$C_{vv}(\tau) \equiv \sum_{i=1}^N \int d\Gamma \rho_{st}(\Gamma) \mathbf{W}_i(t) \cdot \mathbf{W}_i \quad (73)$$

and not of

$$\sum_{i=1}^N \sum_{j=1}^N \int d\Gamma \rho_{st}(\Gamma) \mathbf{W}_i(t) \cdot \mathbf{W}_j. \quad (74)$$

Of course, this has to be taken into account when computing the self-diffusion coefficient by means of DSMC simulations.

Figure 4 shows the velocity autocorrelation function $C_{vv}(\tau)$ for three different values of the coefficient of restitution. It is seen that it decays quite fast to zero, implying the convergence of its time integral and, therefore, the existence of the constant diffusion coefficient. The value of the velocity autocorrelation at each time τ is based on an average of all the times included in the simulation, once the steady state has been reached. In Fig. 5, the same quantity is plotted on a logarithmic scale where an exponential decay for all times is clearly identified.

From the velocity autocorrelation function the self-diffusion coefficient is obtained by means of the Green-Kubo relation (69). Figure 6 shows the ratio of the obtained values $D(T_{HCS}, \alpha)$ to the elastic limit ($\alpha \rightarrow 1$) of the value predicted by the Chapman-Enskog

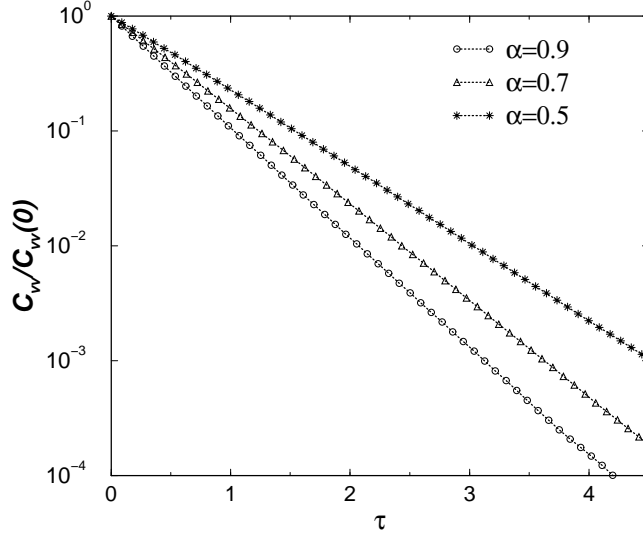


FIG. 5: The same as in Fig. 4 but on a logarithmic scale.

method in the first Sonine approximation $D_0(T_{HCS})$, namely

$$D^*(\alpha) \equiv \frac{D(T_{HCS}, \alpha)}{D_0(T_{HCS})}, \quad (75)$$

$$D_0(T_{HCS}) = \frac{\Gamma(d/2)d}{4\pi^{(d-1)/2}n\sigma^{d-1}} \left(\frac{k_B T_{HCS}}{m} \right)^{1/2}. \quad (76)$$

Also plotted is the theoretical prediction for $D^*(\alpha)$ again in the first Sonine approximation [28],

$$D^*(\alpha) = 4 \left[(1 + \alpha)^2 - \frac{a_2(\alpha)}{16} (4 + \alpha - 3\alpha^2) \right]^{-1}. \quad (77)$$

The agreement between theory and simulation is quite good in all the range of values of α considered, although a systematic deviation, which increases as the value of α decreases, is observed. Self-diffusion in the HCS of a system of inelastic hard spheres ($d = 3$) has been previously studied by means of DSMC in the actual variables, i.e. under continuous cooling, in ref. [28], where the diffusion constant was calculated from the mean-square displacement by means of the (inelastic) Einstein relation and also from the linear response of the system to a density perturbation. The comparison between the numerical results obtained there and the theoretical prediction given by Eq. (77) is very similar to the one presented in Fig. 6. Very recently [29], it has been shown that the agreement improves over the whole range of values of α if $D^*(\alpha)$ is computed in the second Sonine approximation. Although the analysis is restricted to the case of inelastic hard spheres, it seems sensible to expect the same kind of behavior for a system of inelastic hard disks.

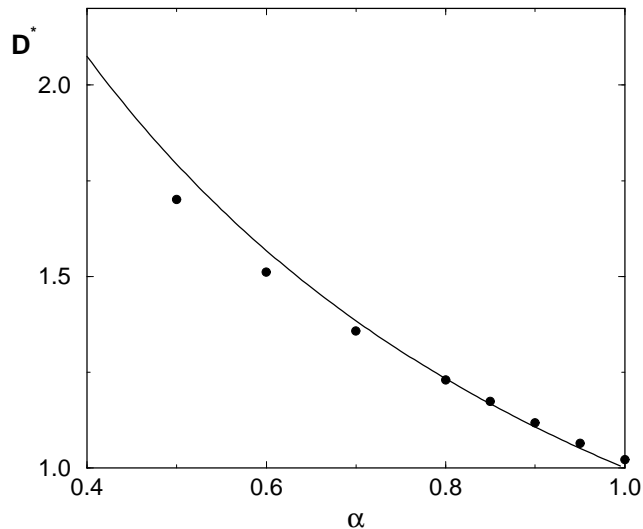


FIG. 6: Dimensionless reduced diffusion coefficient D^* as a function of the coefficient of restitution α . The symbols are from the simulations, while the solid line is the theoretical prediction from the Chapman-Enskog procedure in the first Sonine approximation.

As already mentioned several times, the main feature of the numerical method used here is that it takes advantage of the steady representation of the HCS, removing any limitation on the time on which trajectories of the system may be followed. In addition, let us point out that the analysis of the self-diffusion coefficient based on the velocity autocorrelation function as developed here, is expected to give more accurate results, from a statistical point of view, than those based on the mean square displacement. This is because, while each value of the former in a given trajectory of the system is obtained from an average over all the simulation interval, each value of the latter is obtained from a single evaluation.

VI. DISCUSSION AND CONCLUSION

In this paper, the actual dynamics of a low density granular gas composed of smooth hard inelastic particles has been transformed to another one in which the HCS becomes time-independent. In this way, the need for more or less uncontrolled mechanisms such as internal thermostats in order to get a stationary state is eliminated. The transformation is closely related to the fact that the temperature of the HCS becomes independent from its initial value in the asymptotically long time limit, a property that has not received enough attention up to now. The exact correspondence between both formulations for averages

and time correlation functions has been explicitly established. This requires to consider the kinetic equation for the one-particle distribution function, i.e. the inelastic Boltzmann equation, and also the equation for the two-particle and two-time correlation function in the low density limit. The latter is obtained by extending in a natural way the standard methods of kinetic theory. In particular, it has been shown that the steady temperature directly determines the value of the cooling rate of the system. Then, the DSMC method has been used to measure it and the numerical results have been compared with the theoretical predictions obtained by solving the Boltzmann equation in the first Sonine approximation.

The introduction of the steady representation of the HCS enables the evaluation of the Green-Kubo expressions for the transport coefficients of a dilute granular gas by means of the DSMC method, just as for normal fluids whose particles collide elastically. To put this in a proper context, we have emphasized that the DSMC method is not just a numerical tool to solve the Boltzmann equation, but it formulates an effective N-body dynamics that is expected to be equivalent to the Newtonian one in the low density limit. Moreover, it has the advantage of allowing to incorporate in the own effective dynamics of the particles the symmetry properties of the particular state being simulated. So, it is possible to force the system to stay homogeneous, avoiding the spontaneous development of spacial inhomogeneities associated with the clustering instability. Here this has been illustrated for the simplest case of self-diffusion, whose expression involves the velocity autocorrelation function. The results have been compared with the theoretical prediction obtained by the Chapman-Enskog method and also with previous numerical simulations carried out in the actual dynamics in which the HCS is time-dependent. The study of the remaining Navier-Stokes transport coefficients will be reported elsewhere.

In summary, we believe that the transformed dynamics discussed in this work is of both formal and practical interest for the study of granular fluids in the low density limit. Although we have restricted here ourselves to its application to the HCS, the mapping with the actual dynamics can be easily extended to any arbitrary state.

Acknowledgments

We acknowledge economical support from the Ministerio de Ciencia y Tecnología (Spain) through Grant No. BFM2002-00303 (partially financed by FEDER funds)

APPENDIX A: LOW DENSITY LIMIT OF TIME-CORRELATION FUNCTIONS IN THE HCS

In the low density limit, neglecting three-particle correlations, the function $h_{1/1}$ obeys the equation,

$$\left[\frac{\partial}{\partial t} + \mathbf{v}_1 \cdot \frac{\partial}{\partial \mathbf{r}_1} - K(\mathbf{v}_1, t) \right] h_{1/1}(\mathbf{r}_1, \mathbf{v}_1, t; \mathbf{r}'_1, \mathbf{v}'_1, t') = 0, \quad (\text{A1})$$

where K is the linearized Boltzmann operator

$$K(\mathbf{v}_1, t) = \sigma^{d-1} \int d\mathbf{v}_2 \int d\hat{\boldsymbol{\sigma}} \Theta(\mathbf{v}_{12} \cdot \hat{\boldsymbol{\sigma}}) |\mathbf{v}_{12} \cdot \hat{\boldsymbol{\sigma}}| (\alpha^{-2} b_{\boldsymbol{\sigma}} - 1) (1 + \mathcal{P}_{12}) f_{HCS}(\mathbf{v}_2, t). \quad (\text{A2})$$

The permutation operator \mathcal{P}_{12} interchanges the indexes 1 and 2 of the velocities appearing to its right. The above equation holds for $t > t' > 0$ and it has to be solved with the initial condition

$$h_{1/1}(\mathbf{r}_1, \mathbf{v}_1, t'; \mathbf{r}'_1, \mathbf{v}'_1, t') = g_{2,HCS}(\mathbf{r}_1, \mathbf{v}_1, \mathbf{r}'_1, \mathbf{v}'_1, t') + \delta(\mathbf{r}_1 - \mathbf{r}'_1) \delta(\mathbf{v}_1 - \mathbf{v}'_1) f_{HCS}(\mathbf{v}_1, t'), \quad (\text{A3})$$

$g_{2,HCS}$ being the two-particle one-time correlation function of the HCS. Equation (A1) can be derived by the hierarchy method starting from the pseudo-Liouville equation for a system of inelastic hard spheres or disks. A detailed analysis for the elastic case is presented in ref. [16]. Since the same method can be applied *mutatis mutandis* to the inelastic case, it will be not reproduced here. Now, time and velocities are scaled by

$$\tau = \int_0^t dt' \frac{v_0(t')}{\tilde{v}_{0,st}} \quad (\text{A4})$$

and

$$\mathbf{w} = \frac{\tilde{v}_{0,st}}{v_0(t)} \mathbf{v}, \quad (\text{A5})$$

respectively. We are using the same symbols as in Sec. III since we have seen that in the long time limit the scaling defined by Eq. (A4) is equivalent to that defined by Eq. (25).

The scaled correlation function is

$$\tilde{h}_{1/1}(\mathbf{r}_1, \mathbf{w}_1, \tau; \mathbf{r}'_1, \mathbf{w}'_1, \tau') = \left[\frac{v_0(t)v_0(t')}{\tilde{v}_{0,st}^2} \right]^d h_{1/1}(\mathbf{r}_1, \mathbf{v}_1, t; \mathbf{r}'_1, \mathbf{v}'_1, t') \quad (\text{A6})$$

and, in terms of the new variables, Eq. (A1) becomes

$$\left[\frac{\partial}{\partial \tau} + \mathbf{w}_1 \cdot \frac{\partial}{\partial \mathbf{r}_1} - \Lambda_{st}(\mathbf{w}_1) \right] \tilde{h}_{1/1}(\mathbf{r}_1, \mathbf{w}_1, \tau; \mathbf{r}'_1, \mathbf{w}'_1, \tau') = 0, \quad (\text{A7})$$

valid for $\tau > \tau'$. The operator Λ_{st} is defined by

$$\Lambda_{st}(\mathbf{w}_1) = K_{st}(\mathbf{w}_1) - \omega_0 \frac{\partial}{\partial \mathbf{w}_1} \cdot \mathbf{w}_1, \quad (\text{A8})$$

where K_{st} is the steady linear Boltzmann collision operator

$$K_{st}(\mathbf{w}_1) = \sigma^{d-1} \int d\mathbf{w}_2 \int d\hat{\boldsymbol{\sigma}} \Theta(\mathbf{w}_{12} \cdot \hat{\boldsymbol{\sigma}}) \mathbf{w}_{12} \cdot \hat{\boldsymbol{\sigma}} \left[\alpha^{-2} b_{\sigma}^{-1}(\mathbf{w}_1, \mathbf{w}_2) - 1 \right] (1 + \mathcal{P}_{12}) \tilde{f}_{st}(\mathbf{w}_2). \quad (\text{A9})$$

Integration of Eq. (A7) gives

$$\tilde{h}_{1/1}(\mathbf{r}_1, \mathbf{w}_1, \tau; \mathbf{r}'_1, \mathbf{w}'_1, \tau') = e^{(\tau-\tau')L_B(\mathbf{w}_1)} \tilde{h}_{1/1}(\mathbf{r}_1, \mathbf{w}_1, \tau'; \mathbf{r}'_1, \mathbf{w}'_1, \tau'), \quad (\text{A10})$$

$$L_B(\mathbf{w}_1) = \Lambda_{st}(\mathbf{w}_1) - \mathbf{w}_1 \cdot \frac{\partial}{\partial \mathbf{r}_1}. \quad (\text{A11})$$

The initial condition on the right hand side is

$$\tilde{h}_{1/1}(\mathbf{r}_1, \mathbf{w}_1, \tau'; \mathbf{r}'_1, \mathbf{w}'_1, \tau') = \tilde{g}_{2,HCS}(\mathbf{r}_1, \mathbf{w}_1, \mathbf{r}'_1, \mathbf{w}'_1, \tau') + \delta(\mathbf{r}_1 - \mathbf{r}'_1) \delta(\mathbf{w}_1 - \mathbf{w}'_1) \tilde{f}_{st}(\mathbf{w}_1), \quad (\text{A12})$$

with

$$\tilde{g}_{2,HCS}(\mathbf{r}_1, \mathbf{w}_1, \mathbf{r}'_1, \mathbf{w}'_1, \tau') = \left[\frac{v_0(t')}{\tilde{v}_{0,st}} \right]^{2d} g_2(\mathbf{r}_1, \mathbf{v}_1, \mathbf{r}'_1, \mathbf{v}'_1, t'). \quad (\text{A13})$$

Now the assumption is made that the contribution to Eq. (A10) coming from \tilde{g}_2 can be neglected in the low density limit we are considering. Although there is no explicit proof for this, it is consistent with the hypothesis made to derive the Boltzmann equation. On the other hand, it must be realized that the HCS is not an equilibrium state and, therefore, it can present relevant position and velocity correlations, but we expect them to become negligible for asymptotically small densities. Then, substitution of Eq. (A12) into Eq. (48) yields

$$\begin{aligned} C_{AB}(t, t') &= \int d\mathbf{r}_1 \int d\mathbf{w}_1 \int d\mathbf{r}'_1 \int d\mathbf{w}'_1 a \left[\mathbf{r}_1, \frac{v_0(t)}{\tilde{v}_{0,st}} \mathbf{w}_1 \right] b \left[\mathbf{r}'_1, \frac{v_0(t')}{\tilde{v}_{0,st}} \mathbf{w}'_1 \right] \\ &\quad e^{(\tau-\tau')L_B(\mathbf{w}_1)} \delta(\mathbf{r}_1 - \mathbf{r}'_1) \delta(\mathbf{w}_1 - \mathbf{w}'_1) \tilde{f}_{st}(\mathbf{w}_1) \\ &= \int d\mathbf{r}_1 \int d\mathbf{w}_1 \int d\mathbf{r}'_1 \int d\mathbf{w}'_1 b \left[\mathbf{r}'_1, \frac{v_0(t')}{\tilde{v}_{0,st}} \mathbf{w}'_1 \right] \delta(\mathbf{r}_1 - \mathbf{r}'_1) \delta(\mathbf{w}_1 - \mathbf{w}'_1) \tilde{f}_{st}(\mathbf{w}_1) \\ &\quad e^{(\tau-\tau')\bar{L}_B(\mathbf{w}_1)} a \left[\mathbf{r}_1, \frac{v_0(t)}{\tilde{v}_{0,st}} \mathbf{w}_1 \right] \\ &= \int d\mathbf{r}_1 \int d\mathbf{w}_1 \tilde{f}_{st}(\mathbf{w}_1) b \left[\mathbf{r}_1, \frac{v_0(t')}{\tilde{v}_{0,st}} \mathbf{w}_1 \right] e^{(\tau-\tau')\bar{L}_B(\mathbf{w}_1)} a \left[\mathbf{r}_1, \frac{v_0(t)}{\tilde{v}_{0,st}} \mathbf{w}_1 \right], \quad (\text{A14}) \end{aligned}$$

where \bar{L}_B is the adjoint of L_B and it is given by Eq. (53). The above equation is the same as Eq. (51).

APPENDIX B: GREEN-KUBO EXPRESSION FOR SELF-DIFFUSION FROM THE CHAPMAN-ENSKOG RESULTS

In ref. [28], the self-diffusion coefficient of a dilute granular fluid was obtained from the Boltzmann-Lorentz by the Chapman-Enskog method. Equations (24) and (26) in the above-mentioned reference are

$$D = -\frac{1}{d} \int d\mathbf{v} \mathbf{v} \cdot \mathbf{B}(\mathbf{v}), \quad (\text{B1})$$

where $\mathbf{B}(\mathbf{v})$ is the solution of the integral equation

$$\left(K_{BL} + \zeta_{HCS} T_{HCS} \frac{\partial}{\partial T_{HCS}} \right) \mathbf{B}(\mathbf{v}) = \frac{1}{n_H} \mathbf{v} f_{HCS}(\mathbf{v}), \quad (\text{B2})$$

K_{BL} being the inelastic Boltzmann-Lorentz collision operator

$$K_{BL}(\mathbf{v}) = \sigma^{d-1} \int d\mathbf{v}_1 \int d\hat{\boldsymbol{\sigma}} \Theta(\mathbf{g} \cdot \hat{\boldsymbol{\sigma}}) \mathbf{g} \cdot \hat{\boldsymbol{\sigma}} \left[\alpha^{-2} b_{\boldsymbol{\sigma}}^{-1}(\mathbf{v}, \mathbf{v}_1) - 1 \right] f_{HCS}(\mathbf{v}_1, t). \quad (\text{B3})$$

We introduce dimensionless time and velocity scales by

$$s = \int_0^t dt' \frac{v_0(t')}{\ell}, \quad \mathbf{c} = \frac{\mathbf{v}}{v_0(t)}. \quad (\text{B4})$$

In terms of them, Eq. (B2) becomes

$$\left(K_{BL,c} - \frac{\zeta_0}{2} \frac{\partial}{\partial \mathbf{c}} \cdot \mathbf{c} \right) \tilde{\mathbf{B}}(\mathbf{c}) = \mathbf{c} \chi_{HCS}(\mathbf{c}), \quad (\text{B5})$$

with

$$\tilde{\mathbf{B}}(\mathbf{c}) = \frac{v_0^d(t)}{\ell} \mathbf{B}(\mathbf{v}) \quad (\text{B6})$$

and

$$K_{BL,c}(\mathbf{c}) = \frac{\ell}{v_0(t)} K_{BL}(\mathbf{v}). \quad (\text{B7})$$

The formal solution of Eq. (B5) can be written as

$$\tilde{\mathbf{B}}(\mathbf{c}) = - \int_0^\infty ds e^{s\Lambda_{BL,c}(\mathbf{c})} \mathbf{c} \chi_{HCS}(\mathbf{c}), \quad (\text{B8})$$

$$\Lambda_{BL,c}(\mathbf{c}) = K_{BL,c}(\mathbf{c}) - \frac{\zeta_0}{2} \frac{\partial}{\partial \mathbf{c}} \cdot \mathbf{c}. \quad (\text{B9})$$

Substitution of Eq. (B8) into Eq. (B1) gives

$$\begin{aligned} D &= \frac{v_0(t)\ell}{d} \int_0^\infty ds \int d\mathbf{c} \mathbf{c} \cdot e^{s\Lambda_{BL,c}(\mathbf{c})} [\mathbf{c} \chi_{HCS}(\mathbf{c})] \\ &= \frac{v_0(t)\ell}{d} \int_0^\infty ds \int d\mathbf{c} \left[e^{s\bar{\Lambda}_{BL,c}(\mathbf{c})} \mathbf{c} \right] \cdot \mathbf{c} \chi_{HCS}(\mathbf{c}), \end{aligned} \quad (\text{B10})$$

where $\bar{\Lambda}_{BL,c}(\mathbf{c})$ is the adjoint of $\Lambda_{BL,c}(\mathbf{c})$,

$$\bar{\Lambda}_{BL,c}(\mathbf{c}_1) = \int d\mathbf{c}_2 \chi_{HCS}(\mathbf{c}_2) \int d\hat{\boldsymbol{\sigma}} \Theta(\mathbf{c}_{12} \cdot \hat{\boldsymbol{\sigma}}) \mathbf{c}_{12} \cdot \hat{\boldsymbol{\sigma}} [b_{\boldsymbol{\sigma}}(\mathbf{c}_1, \mathbf{c}_2) - 1] + \frac{\zeta_0}{2} \mathbf{c}_1 \cdot \frac{\partial}{\partial \mathbf{c}_1}. \quad (\text{B11})$$

-
- [1] *Granular gases*, edited by T. Pöschel and S. Luding (Springer-Verlag, Berlin, 2001).
- [2] I. Goldhirsch and G. Zanetti, Phys. Rev. Lett. **70**, 1619 (1993); I. Goldhirsch, M.L. Tan, and G. Zanetti, J. Sci. Comput. **8**, 1 (1993).
- [3] A. Kudrolli, M. Wolpert, and J.P. Gollup, Phys. Rev. Lett. **78**, 1383 (1997).
- [4] H.J. Schlichting and V. Nordmeier, Math. Naturwiss. Unterr. **49**, 323 (1996); J. Eggers, Phys. Rev. Lett. **83**, 5322 (1999); K. van der Weele, D. van der Meer, and D. Lohse in *Granular Gas Dynamics*, edited by T. Pöschel and N. Brilliantov (Springer-Verlag, Berlin, 2003).
- [5] J.J. Brey, F. Moreno, R. García-Rojo, and M.J. Ruiz-Montero, Phys. Rev. E **65**, 011305 (2002).
- [6] E. Livne, B. Meerson, and P.V. Sasorov, Phys. Rev. E **65**, 021302 (2002); J.J. Brey, M.J. Ruiz-Montero, F. Moreno, and R. García-Rojo, Phys. Rev. E **65**, 061302 (2002); M. Argentina, M. Clerk, and R. Soto, Phys. Rev. Lett. **89**, 044301 (2002).
- [7] A.D. Rosato, T. Vreeland, Jr., and F.B. Prinz, Int. Mater. Rev. **36**, 45 (1991); J. Duran, J. Rajchenbach, and E. Clément, Phys. Rev. Lett. **70**, 2431 (1993); A.P.J. Breu, H.-M. Ensner, C.A. Kruelle, and I. Rehberg, Phys. Rev. Lett. **90**, 014302 (2003).
- [8] P.B. Umbanhowar, F. Melo, and H.L. Swinney, Nature **382**, 793 (1996).
- [9] J.J. Brey, J.W. Dufty, C.S. Kim, and A. Santos, Phys. Rev. E **58**, 4638 (1998).
- [10] V. Garzó and J.W. Dufty, Phys. Rev. E **59**, 5895 (1999).
- [11] I. Goldhirsch and T.P.C. van Noije, Phys. Rev. E **61**, 3241 (2000).
- [12] J.W. Dufty and J.J. Brey, Physica A **109**, 433 (2002).
- [13] R. Soto and M. Mareschal, Phys. Rev. E **63**, 041303 (2001).
- [14] J.F. Lutsko, Phys. Rev. E **63**, 061211 (2001).
- [15] S. McNamara and W.R. Young, Phys. Rev. E, **50**, Phys. Rev. E **50**, R28 (1994); *ibid* **53**, 5089 (1996).
- [16] M.H. Ernst and E.G.D. Cohen, J. Stat. Phys. **25**, 153 (1981).

- [17] G. Bird *Molecular Gas Dynamics and the Direct Simulation of Gas Flows*, (Clarendon Press, Oxford, 1994).
- [18] A. Goldstein and M. Shapiro, *J. Fluid Mech.* **282**, 75 (1995).
- [19] J.J. Brey, J.W. Dufty, and A. Santos, *J. Stat. Phys.* **87**, 1051 (1997).
- [20] P.K. Haff, *J. Fluid Mech.* **134**, 401 (1983).
- [21] T.P.C. van Noije and M.H. Ernst, *Granular Matter* **1**, 57 (1998).
- [22] J.J. Brey, M.J. Ruiz-Montero, and D. Cubero, *Phys. Rev. E* **54**, 3664 (1996).
- [23] J.J. Brey, M.J. Ruiz-Montero, and D. Cubero, *Phys. Rev. E* **60**, 3150 (1999).
- [24] A.L. García, *Numerical Methods for Physics*, (Prentice Hall, Englewood Cliffs NJ, 2000).
- [25] J. Lutsko, J.J. Brey, and J.W. Dufty, *Phys. Rev. A* **65**, 051304 (2002).
- [26] J.W. Dufty and J.J. Brey, *Phys. Rev. E* **53**, 030302 (2003).
- [27] J.J. Brey, J.W. Dufty, and M.J. Ruiz-Montero in *Granular Gas Dynamics*, edited by T. Pöschel and N. Brilliantov (Springer-Verlag, Berlin, 2003).
- [28] J.J. Brey, M.J. Ruiz-Montero, D. Cubero, and R. García-Rojo, *Phys. Fluids* **12**, 876 (2000).
- [29] V. Garzó and J.M. Montanero, *Phys. Rev. E*, to appear (2003).